BULETINUL INSTITUTULUI POLITEHNIC DIN IAŞI
Publicat de
Universitatea Tehnică „Gheorghe Asachi” din Iaşi
Volumul 66 (70), Numărul 4, 2020
Secţia
CONSTRUCŢII. ARHITECTURĂ

THE INFLUENCE OF THE RC BEAMS CROSS SECTION ON THE DISSIPATIVE SEISMIC RESPONSE OF A MOMENT RESISTING RC FRAME SYSTEM

BY

ION SOCOCOL*, PETRU MIHAI, IONUȚ-OVIDIU TOMA, IOANA OLTEANU-DONȚOV and VASILE-MIRCEA VENGHIAC

"Gheorghe Asachi" Technical University of Iași,
Faculty of Civil Engineering and Building Services, Iași, Romania

Received: October 10, 2020
Accepted for publication: November 15, 2020

Abstract. The idealized seismic response of reinforced concrete frame structures implies the occurrence of energy dissipation mechanisms by means of plastic deformations. These plastic deformations are expected to occur at the end sections of the beams and at the base of the ground-floor column. This, in turn, leads to the optimum deformation of the structure and the formation of the global distribution of the plastic hinges. Taking into account the influence of the concrete strength class and that of the longitudinal reinforcement ratio in the columns on the seismic behaviour of RC moment resisting frame structures, the present paper aims at investigating the contribution of the beam cross-section to the formation of the plastic hinges. The non-linear static analyses using the finite element method were conducted by means of the ATENA software for three distinct RC moment resisting frame models with rigid, normal and flexible beams designed according to the prescription of the current norms. While the model with flexible beams exhibited the idealized failure mechanism, its applicability in design practice is rather reduced given its high flexibility. On the other hand, for the model incorporating rigid beams it was observed that the plastic deformations tended to concentrate at the end sections of the columns.

*Corresponding author; *e-mail*: ion.sococol@tuiasi.ro

Keywords: dissipative structural elements; dissipative zones/ areas; RC rigid beams; RC flexible beams; static nonlinear analysis.

1. Introduction

The columns and the beams in a moment resisting frame structure are generally subjected to moment reversals during seismic excitations. Current design codes try to ensure that adequate strength is maintained even under cyclic loading scenarios involving large lateral displacements by imposing that the flexural yielding occurs at the end of beams, at the face of the beam-column joint, and that the columns are still working in the linear elastic range.

The performance-based seismic design approach requires the modeling of all possible sources of flexibility in the frame structure when trying to assess the frame response to cyclic loading scenarios (Birely *et al.*, 2012). It is commonly agreed that the damage caused by earthquakes in reinforced concrete frame structures tends to concentrate in the area of the joints between the linear elements (Navarro-Gomez and Bonet, 2019). The damage is initiated by the crushing and spalling of the concrete cover, followed by the yielding of the longitudinal reinforcement and, sometimes, the failure of the shear reinforcement due to inadequate detailing or construction errors. This leads to large residual deformations in the structure after the seismic event and repairing measures need to be taken with significant economic losses.

The paper presents the results obtained by means of numerical investigations on the influence of the RC beams cross-section on the dissipative seismic response of a moment resisting frame system. The present research is a continuation of the wider research program meant to assess the influencing factors on the location and development of the plastic hinges in RC moment resisting frame structures.

A half-scale reinforced concrete frame model following all rules of similarity was used for generating the numerical model (Sococol *et al.*, 2020a), as shown in Fig. 1. The same model was used to assess the improved seismic response for a higher concrete strength class (Sococol *et al.*, 2020a) and a higher longitudinal reinforcement ratio for RC columns (Sococol *et al.*, 2020b) during the previous stage of the research program. These analytical aspects represented the first two steps in specifying the optimal RC frame layout to be tested on the shake table. The next step is the current research study on optimal RC beams cross sections for adequate dissipative seismic response.

2. Main Research Parameter

The main parameter considered at this stage of the research was the cross-section of the beams. The height of the beams was determined based on the preliminary design stage empirical equations considering the structural stiffness requirement (Kripka *et al.*, 2015):

i) for h_B=1/8L condition – rigid RC longitudinal beams (Table 1, Fig. 2) – model M_5;

ii) for h_B=1/12L condition – normal RC beams (Table 1, Fig. 2) – model K_5;

iii) for h_B=1/16L condition – ductile / flexible RC beams (Table 1, Fig. 2) – model Z_5;

where h_B was the height of the beam and L was the clear span.

For each of the three models shown in Fig. 1 and Fig. 2 all possible failure mechanisms were considered in the numerical model: concrete cracking in tension, concrete crushing in compression and yielding of the longitudinal reinforcement (Bitencourt *et al.*, 2018; Leppanen *et al*., 2020). The failure mechanisms of RC structures is quite difficult to be captured due to the complex phenomena that take place at the material level (Leppanen *et al*., 2020). However, careful modelling of the geometry and the use of the appropriate material models as part of the FEM analysis (ATENA software, 2015) could lead to quite realistic simulations of the real failure patterns (Sousa Jr. and Muniz, 2006; Sciegaj *et al*., 2020).

Previous reports available in the scientific literature (Zidonis, 2013; Bednarski *et al.*, 2015; Thamrin *et al*., 2017; Almahmood *et al.*, 2020; Gao *et al.*, 2020; Gribniak *et al.*, 2020; Hassan *et al.*, 2020; Tayeh *et al.*, 2020) underline the importance of the research direction highlighted in the present study.

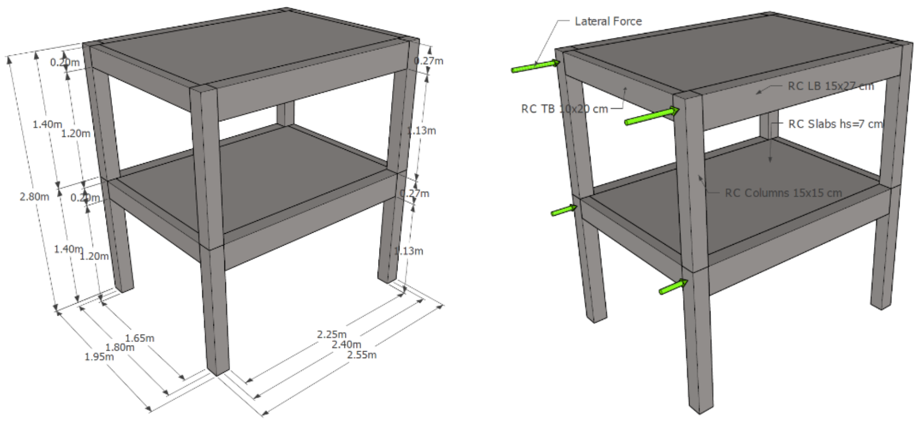

(*a*) (*b*)

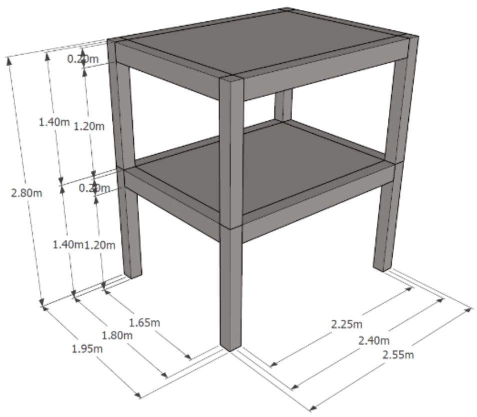

(*c*)

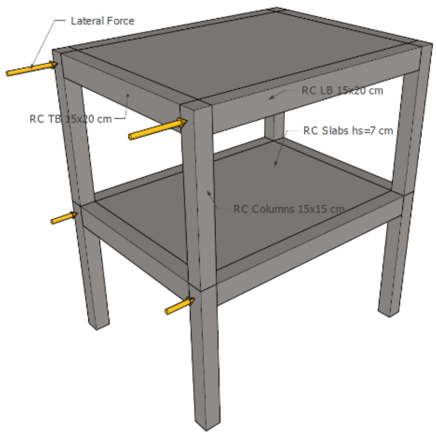

(*d*)

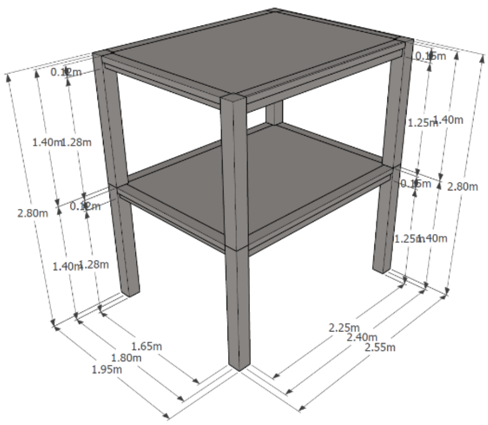

(*e*)

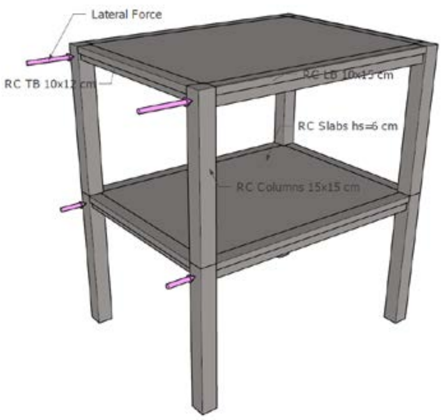

(*f*)

Fig. 1 – (*a*) Structure dimensions of the M_5 RC moment resisting frame model with longitudinal rigid beams; (*b*) Pushover loading consideration for M_5 RC frame system; (*c*) Structure dimensions of the K_5 moment resisting RC frame model; (*d*) Pushover loading consideration for K_5 RC frame system; (*e*) Structure dimensions of the Z_5 moment resisting RC frame model with ductile beams; (*f*) Pushover loading consideration for Z_5 RC frame system.

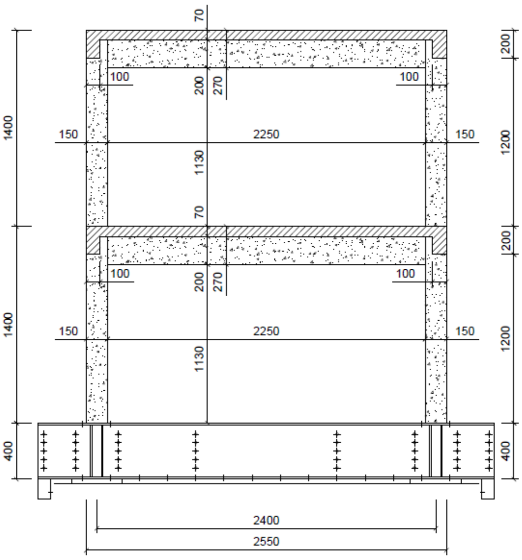
70
200
100
200
270
100
1400
150
2250
150
1200
1130
70
200
100
200
270
100
1400
150
2250
150
1200
1130
400
400
2400
2550

(*a*)

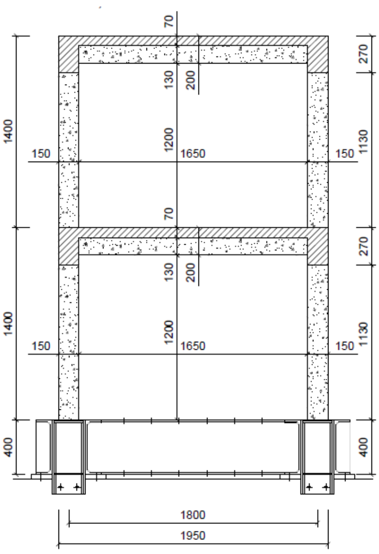
70
270
130
200
1400
150
1200
1650
150
1130
70
270
130
200
1400
150
1200
1650
150
1130
400
400
1800
1950

(*b*)

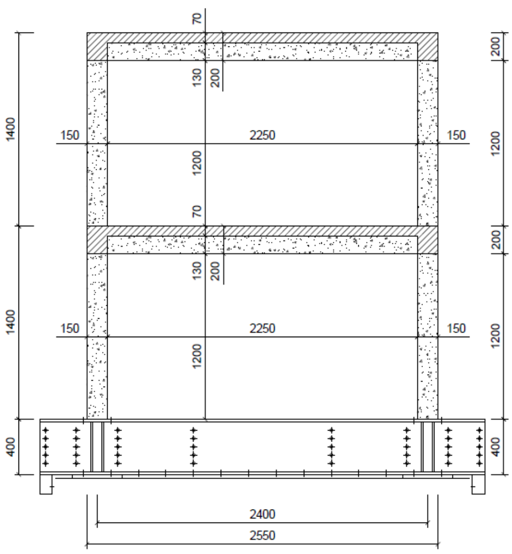
70
200
130
200
1400
150
2250
150
1200
1200
70
200
130
200
1400
150
2250
150
1200
1200
400
400
2400
2550

(*c*)

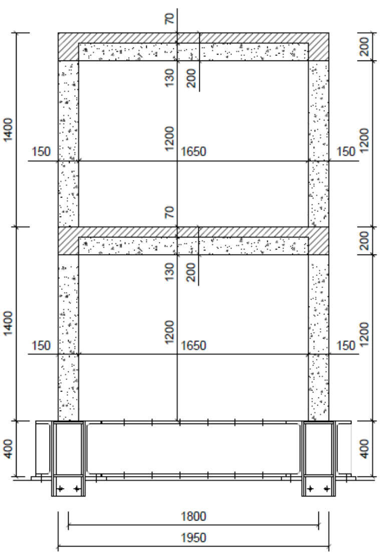
70
200
130
200
1400
150
1200
1650
150
1200
70
200
130
200
1400
150
1200
1650
150
1200
400
400
1800
1950

(*d*)

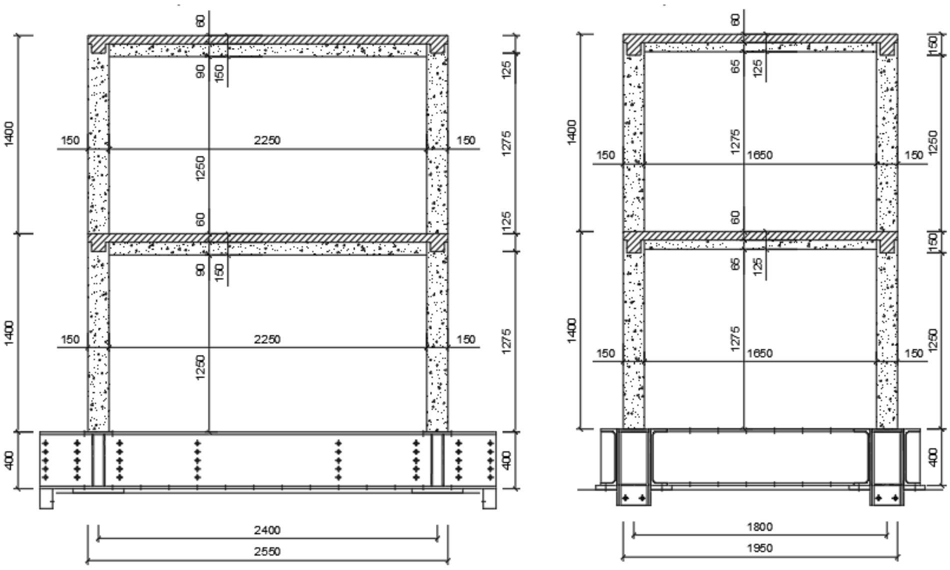

(*e*) (*f*)

Fig. 2 – Representation of longitudinal and transverse cross sections for: (*a*, *b*) M_5 RC moment resisting frame model with longitudinal rigid beams (see Fig. 1 (*a*)); (*c*, *d*) K_5 RC moment resisting frame system (see Fig. 1 (*c*)); (*e*, *f*) Z_5 moment resisting RC frame model with ductile beams (see Fig. 1(*e*)) (for all RC frame systems see Table 1).

3. Geometry of the Model and Loading Conditions

The analytical study presented in this paper represents a continuation of the nonlinear static analyses for the optimal RC experimental frame model design to be tested on the shake table (Sococol *et al.*, 2020a; Sococol *et al.*, 2020b). The geometry of the model, shown in Fig. 2, is similar to the one reported in earlier research works:

i. the in-plane dimensions of the ½ scale RC frame system are L=2.4 m, B=1.8 m;
ii. the height regime: GF+1S. It falls into the category of small-scale buildings according to (Ishiyama, 2011);
iii. storey height: h_{st}=1.4 m; H_{tot}=2.8 m;
iv. the building is considered to belong to the importance class III, according to P100-1 (P100-1, 2013);
v. the type of structure: pure RC frame (without non-structural components to avoid their effects (Sococol *et al.*, 2019a));
vi. structural ductility class: DCH, according to P100-1 (P100-1, 2013) and based on the research works performed by (Postelnicu, 2012; Budescu and Ciongradi, 2014; Stratan, 2014; Sococol *et al.*, 2019b).

The cross-sectional dimensions of the columns were constant for all three considered numerical models. The thickness of the slab however, changed from 7 cm for M_5 and K_5 models to 6 cm for the Z_5 model.

Both longitudinal and transversal beams were reinforced by means of 4 $4\phi10$ BST 500S steel bars. The RC columns were reinforced by $4\phi14$ BST 500S steel bars in order to use the optimum longitudinal reinforcement ratio reported in earlier research works by Sococol *et al.* (2020b).

The shear reinforcement for columns and beams consisted of $\phi4$ BST 500M stirrups positioned at 5 cm in critical zones and 10 cm in other areas. The critical zones were considered to be the end of the beams (one third of the clear span) as well as the entire height of the columns (Sococol *et al.*, 2020a; Sococol *et al.*, 2020b). The reinforcement layout and the generated FEM model are shown in Fig. 3.

Table 1
Parameters Considered in Numerical Analysis for the Moment Resisting RC Frame Models

<table>
<tr><td colspan="6">RC longitudinal rigid beams preliminary design condition: h_B=1/8L</td></tr>
<tr><td>CSC</td><td>NSC</td><td>RC C
(15x15 cm)</td><td>RC LB
(15x27 cm)</td><td>RC TB
(10x20 cm)</td><td>RC S
(h_s=7 cm)</td></tr>
<tr><td>C20/25</td><td>M_5</td><td>$4\phi14$</td><td>$4\phi10$</td><td>$4\phi10$</td><td>$\phi6$</td></tr>
<tr><td colspan="6">RC beams preliminary design condition: h_B=1/12L</td></tr>
<tr><td>CSC</td><td>NSC</td><td>RC C
(15x15 cm)</td><td>RC LB
(15x20 cm)</td><td>RC TB
(15x20 cm)</td><td>RC S
(h_s=7 cm)</td></tr>
<tr><td>C20/25</td><td>K_5</td><td>$4\phi14$</td><td>$4\phi10$</td><td>$4\phi10$</td><td>$\phi6$</td></tr>
<tr><td colspan="6">*RC ductile beams preliminary design condition: h_B=1/16L</td></tr>
<tr><td>CSC</td><td>NSC</td><td>RC C
(15x15 cm)</td><td>RC LB
(10x15 cm)</td><td>RC TB
(10x12 cm)</td><td>RC S
(h_s=6 cm)</td></tr>
<tr><td>C20/25</td><td>Z_5</td><td>$4\phi14$</td><td>$4\phi10$</td><td>$4\phi10$</td><td>$\phi6$</td></tr>
<tr><td colspan="6">Note: CSC – Concrete Strength Class; NSC – Numerical Simulation Code; RC – Reinforced Concrete; C – Columns; LB – Longitudinal Beams; TB – Transverse Beams; S –Slabs; h_s – RC slabs thickness; h_B – RC beams thickness.
* Minimum beam height requirement (P100-1, 2013).</td></tr>
</table>

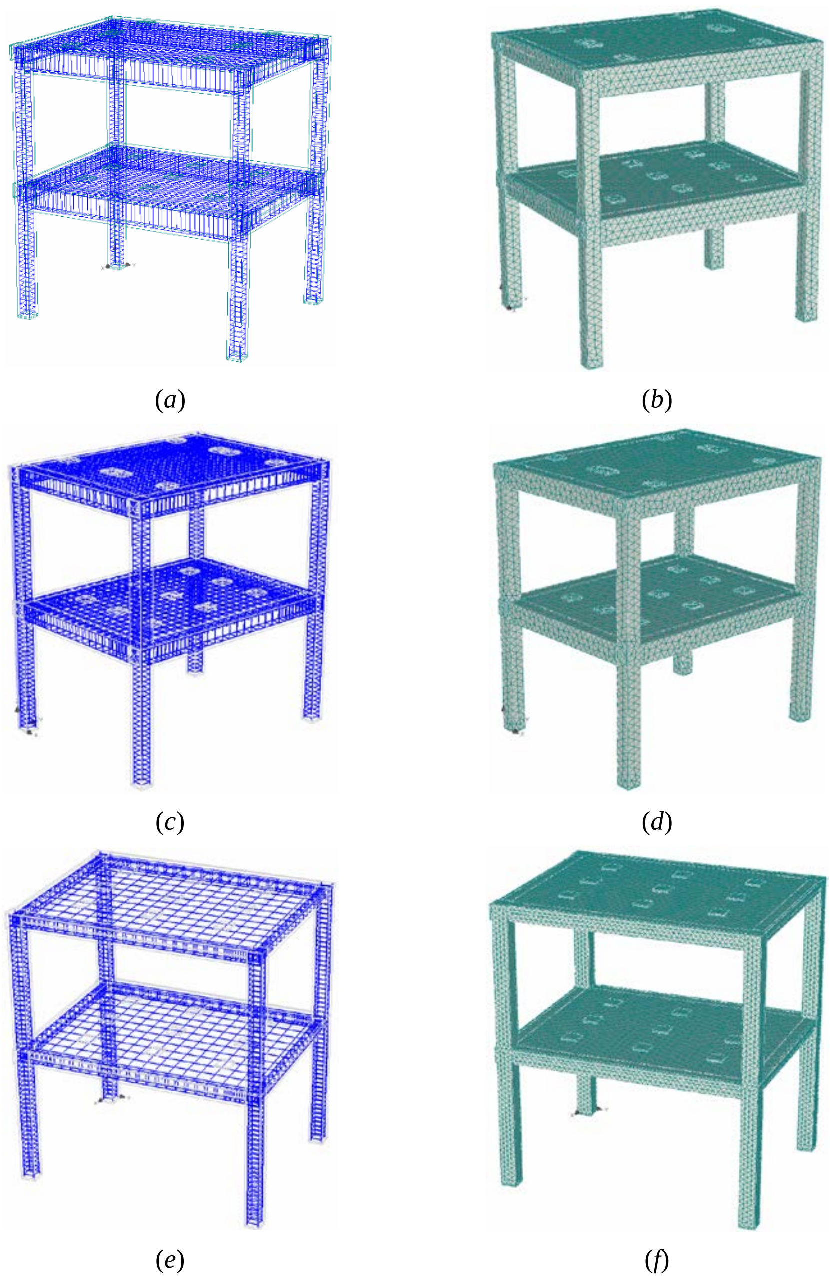

Fig. 3 – (*a*) Steel reinforcement layout in M_5 model; (*b*) Structural mesh discretization for M_5 model; (*c*) Steel reinforcement layout in K_5 model; (*d*) Structural mesh discretization for K_5 model; (*e*) Steel reinforcement layout in Z_5 model; (*f*) Structural mesh discretization for Z_5 moment resisting RC frame system (Capua and Mari, 2007).

Lateral loads with implicit horizontal values were considered for each model. The simplified 2 Degrees of Freedom Models (2DoFM) lateral are shown in Fig. 4. The magnitude of the lateral loads was directly influenced by the geometry of the models, Fig. 2. The interaction between the steel reinforcement and the concrete material was also accounted for in the numerical model. A perfect bond was assumed for the initial, unstressed, conditions.

The output parameter data correspond for all moment resisting RC frame models in following form enumeration (Sococol *et al.*, 2020a; Sococol *et al.*, 2020b): ultimate lateral displacements and forces, total strains, principal fracture strains as well as crack patterns due to the lateral displacements.

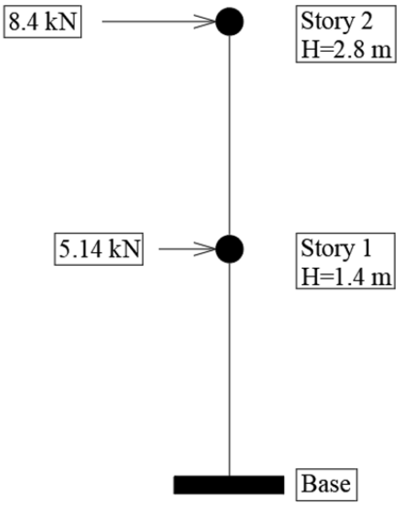

(*a*)

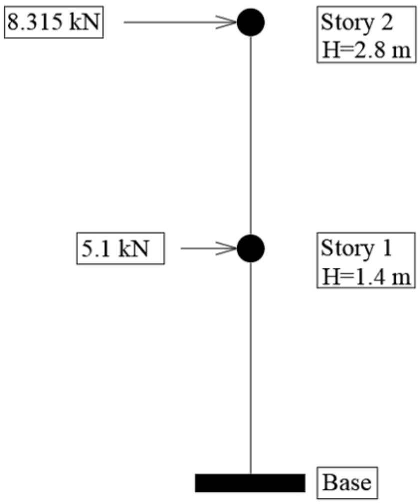

(*b*)

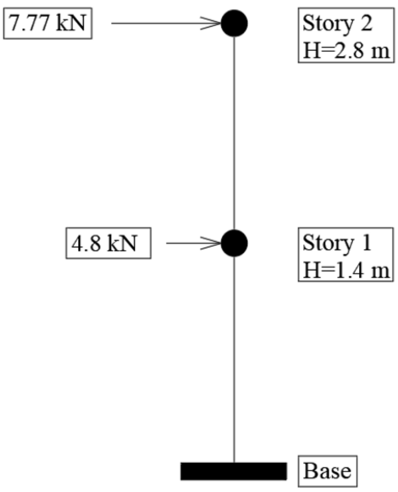

(*c*)

Fig. 4 – Representation of the discrete system with lateral load consideration in the longitudinal direction for: (*a*) M_5 (see Fig. 1 (*b*)); (*b*) K_5 (see Fig. 1 (*d*)); (*c*) Z_5 (see Fig. 1 (*f*)) moment resisting RC frame model.

4. Nonlinear Static Analysis Results

As previously mentioned, the magnitude of the lateral loads was influenced by the geometry of the model which resulted in modified self-weight depending on the cross-sectional dimensions of the beams and slabs. The loads were evaluated in accordance with P100-1 code (P100-1, 2013). The obtained results are summarized in Fig. 5 – Fig. 8, as well as Table 2. The failure mechanisms in terms of tensile macrocracking of concrete, the compressive strains of concrete and the tensile strains of steel were also assessed (Schlappal *et al.*, 2020). Therefore, a set of observations could be made following the FEM analyses on the influence of the beams cross-sections on the global seismic response of the considered moment resisting RC frame structure (Budescu and Ciongradi, 2014; Sococol *et al.*, 2019b),

The M_5 model exhibits the smallest lateral displacement, $D_{M\_5} = 0.0246$ m as shown in Fig. 5, but at the same time, the highest lateral force was required to reach that displacement $F_{max} = 48.3$ kN, as presented in Fig. 6 (Sococol *et al.*, 2020b). A possible explanation could be that the reigid longitudinal beams lead to the occurrence of plastic deformations in the frame joint by means of micro- and macro-cracking of the concrete associated to te yielding of the longitudinal reinforcement from the columns (Fig. 7 (*a*, *b*)). According to previous research work of Sococol *et al.* (2020b), the principal fracture strains exceeded the ultimate axial strains limit of the concrete ($\varepsilon_{PFSM} = 0.2524 > \varepsilon_{cu,c} = 0.0035$) (Table 2, Fig. 8 and Fig. 7 (*b*)) as well as the ultimate axial strain limit for steel ($\varepsilon_{PFSM} = 0.2524 > \varepsilon_{uk} = 0.075$) (Sococol *et al.*, 2019b).

Moreover, the M_5 RC frame model developed the so-called RC rigid „beams-node-slabs" common block (Sococol *et al.*, 2019c) with significant influences on the local deformations due to the induced shear stresses (Ayensa *et al.*, 2019; Yuan and Wang, 2019; Karimipour and Edalati, 2020; Wang *et al.*, 2020). Therefore, the ideal failure mechanism assumed for the lateral loading scenarios did not occur (Jokubaitis *et al.*, 2013; Simeng and Huixiang, 2018).

The ultimate lateral load for the K_5 moment resisting RC frame system was $F_{K\_5} = 43.654$ kN, as seen from Fig. 6, due to a reduced or decreased structural stiffness. The decrease in the structural stiffness due to smaller cross-sections for the beams leads to the occurrence of an energy dissipation mechanism by means of lateral displacements, $D_{K\_5} = 0.0276$ m (Fig. 5). Moreover, it was observed that the plastic hinge area extended well outside the joint area, the latter being heavily cracked (Fig. 7 (*c*, *d*)). The principal fracture strains did not exceed the ultimate specific strains limit of the concrete in compression, $\varepsilon_{PFSM} = 0.0271 < \varepsilon_{cu,c} = 0.0035$ (see Table 2, Table 3, Fig. 8 and Fig. 7 (*d*)), as well as tensile strain of steel $\varepsilon_{PFSM} = 0.0271 < \varepsilon_{uk} = 0.075$ (see Table 2, Table 3, Fig. 8 and Fig. 7 (*d*)) at the end sections of the beams.

However, the RC beams in the considered configuration still contribute to the formation of the “beam-slab-joint” rigid block (Sococol *et al.*, 2019c; Sococol *et al.*, 2020a; Sococol *et al.*, 2020b). This leads to a limited / partially restrained rotation of the beam ends and, consequently, a limited energy dissipation capacity (Fig. 7(*d*)) with dignificant cracking of the reinforced concrete cross sections (Simao *et al*., 2016) in the areas where the occurrence of the plastic dissipation mechanisms are expected, according to current design norms (EC 8, 2004; P100-1, 2013).

The more flexible beams from Z_5 model lead to the best structural response from the investigated cases. Although the lateral force is the lowest, F_{min} = 37.418 kN (Fig. 6), the exhibited lateral displacement is almost twice as large as the corresponding displacements for the other two considered models,ns of the beams (Fig. 7(*e*, *f*)). The beams still work together with the slab, exhibiting the same rotation as it can be seen from the cracking pattern presented in Fig. 7(*e*). From the point of view of the values for the **P**rincipal **F**racture **S**trains **M**ax (Fig. 8) and **T**otal **S**trains **E**ps zz (Fig. 9), they are better than the values obtained for the other two numerical models with concrete cracking ε_{TSE} = 0.004155 > $\varepsilon_{cu,c}$ = 0.0035 (Table 2, Fig. 9 and Fig. 7(*e*)) and yielding of the longitudinal reinforcement at the end sections of the beams ε_{PFSM} = 0.0601 < ε_{uk} = 0.075 (Table 2, Table 3, Fig. 8 and Fig. 7(*f*)) but without reaching the ultimate limit strain. Thus, the Z_5 moment resisting RC frame system develops the ideal failure pattern with crushing of the concrete at the same time with the yielding of the tensioned steel reinforcement at the end sections of the beams.

Table 2
Analysis Results for the M_5, K_5 and Z_5 Moment Resisting RC Frame Systems

CSC	NSC	ULD [m]	ULF [kN]	TSE	PFSM
C20/25	*M_5*	*0.0246*	*48.3*	*0.002637*	*0.02524*
C20/25	*K_5*	*0.0276*	*43.654*	*0.002486*	*0.0271*
C20/25	*Z_5*	*0.0634*	*37.418*	*0.004155*	*0.0601*

Table 3
Characteristic Values for the C20/25 Concrete and S500 Steel Reinforcement Strains (EC 2, 2006; Kiss and Onet, 2008)

Ultimate compressive strain $\varepsilon_{cu,c}$ (‰) of C20/25 concrete	
Concrete class	*Ultimate compressive strain $\varepsilon_{cu,c}$ (‰)*
C20/25	*3.5*

Ultimate tensile strain ε_{uk} (%) of S500 steel reinforcement			
Steel grade	*Commercial deisgnation*	*Ductility class*	*Ultimate tensile strain ε_{uk} (%)*
S500	*Bst 500S*	*C*	*≥ 7.5*

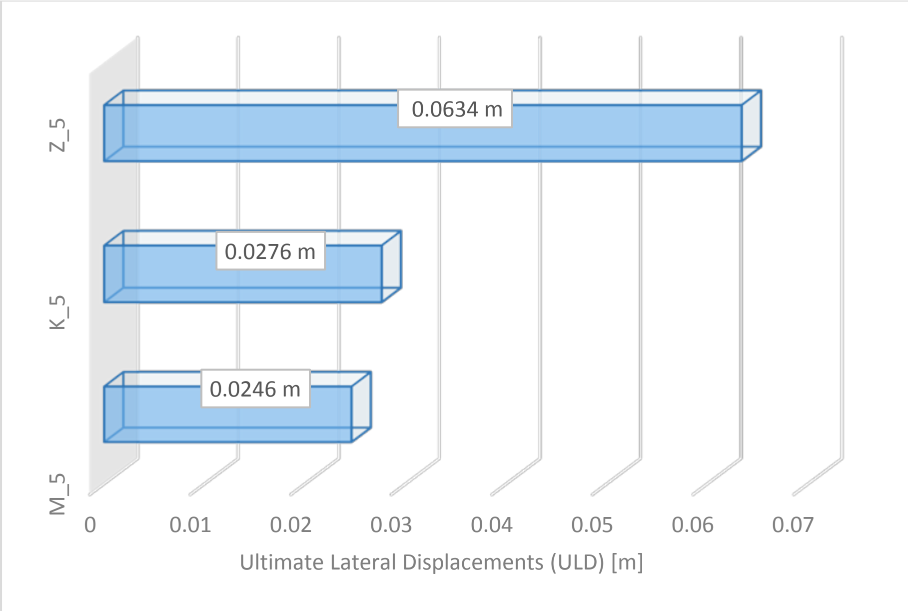

Fig. 5 – Influence of the RC beams cross sections on the **U**ltimate **L**ateral **D**isplacements (ULD) seismic response for M_5, K_5 and Z_5 moment resisting RC frame systems.

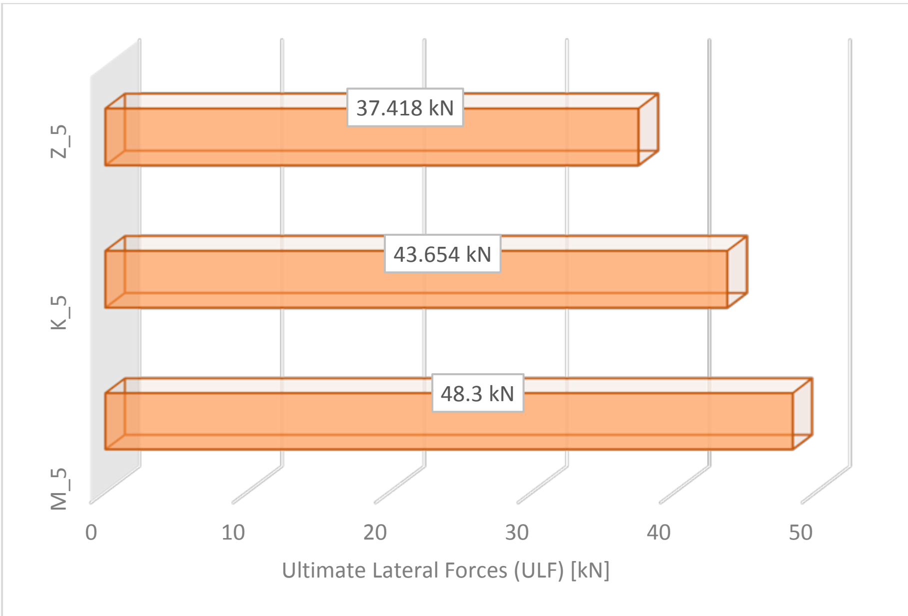

Fig. 6 – Influence of the RC beams cross sections on the **U**ltimate **L**ateral **F**orces (ULF) lateral (seismic) response for M_5, K_5 and Z_5 moment resisting RC frame systems.

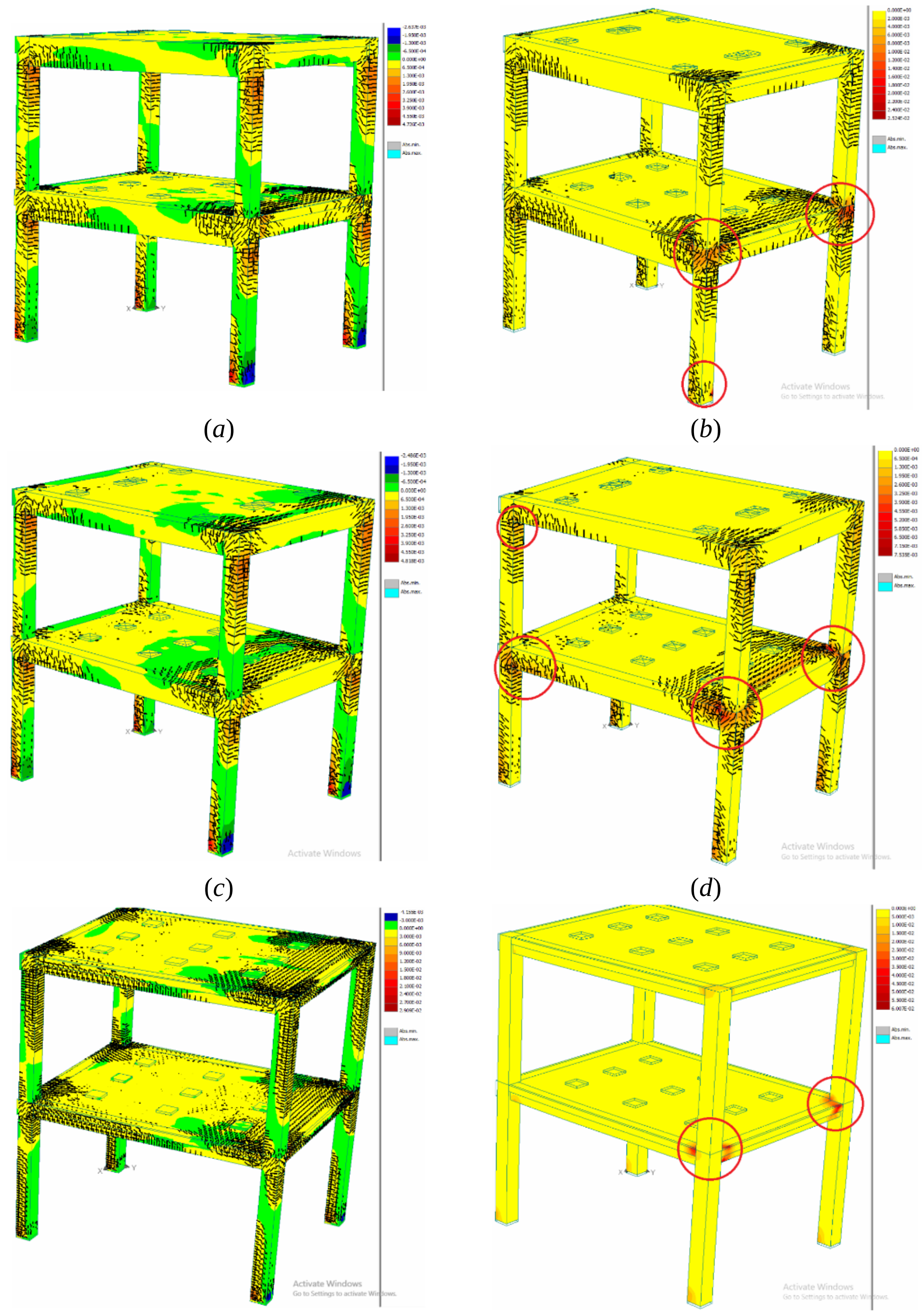

(*a*) (*b*) (*c*) (*d*) (*e*) (*f*)

Fig. 7 – (*a*), (*c*), (*e*) **T**otal **S**train **E**pszz (TSE) for M_5, K_5 and Z_5 moment resisting RC frames; (*b*), (*d*), (*f*) **P**rincipal **F**racture **S**trains **M**ax (PFSM) for M_5, K_5 and Z_5 moment resisting RC frame models.

x

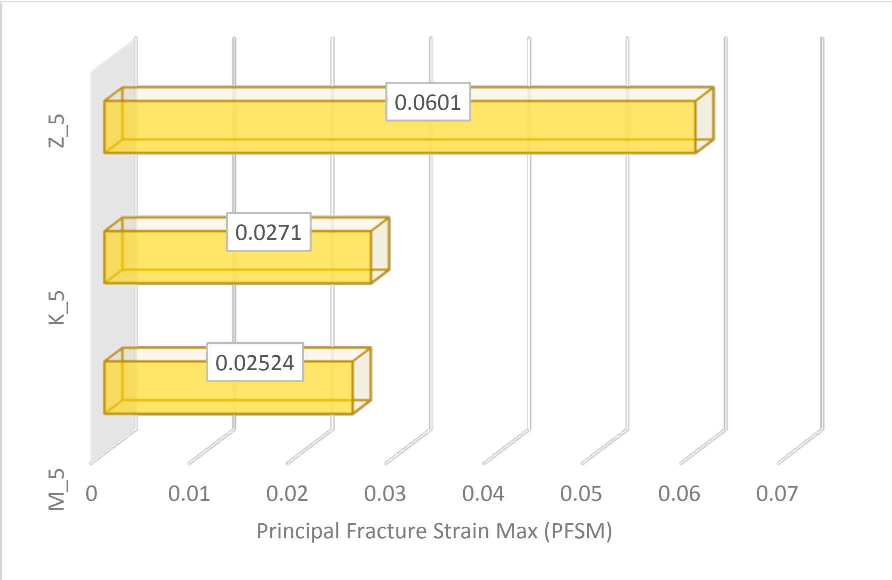

Fig. 8 – Influence of the RC beams cross sections on the lateral seismic response in **P**rincipal **F**racture **S**trains **M**ax (PFSM) for M_5, K_5 and Z_5 RC moment resisting frame models (see Table 2 and Fig. 7).

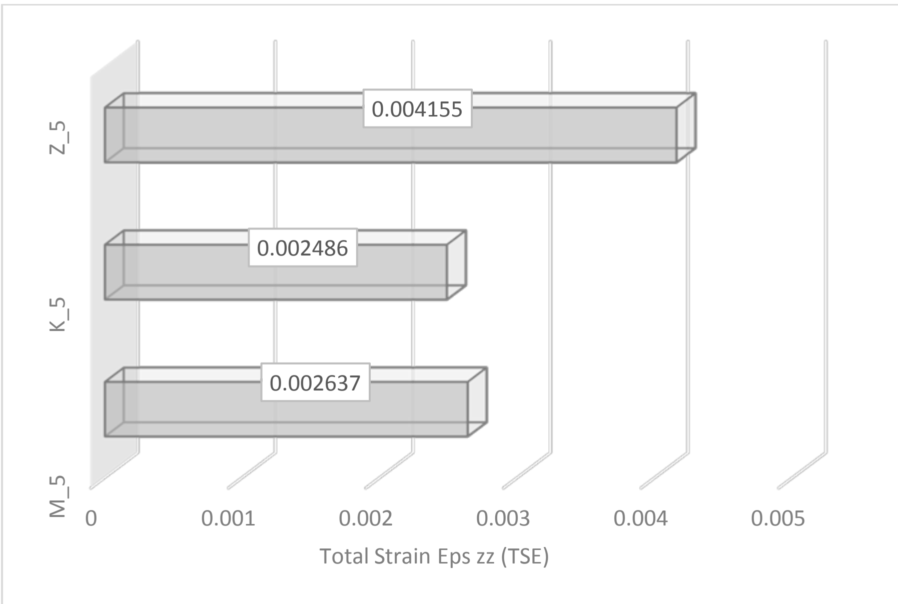

Fig. 9 – Influence of the RC beams cross sections on the seismic response in **T**otal **S**trains **E**ps zz (TSE) for M_5, K_5 and Z_5 RC frame models (see Table 2, Fig. 7).

5. Conclusions

The non-linear static analyses conducted by means of ATENA software related to the influence of the beam cross-section on the seismic behaviour of RC moment-resisting frame structures rendered evident the idealized ductile failure mechanism specified in the current seismic design norms.

Based on the obtained results it can be concluded that the Z_5 model, the one with the flexible beams designed according to the lower limit of the cross-section height, shows the most favourable response to lateral loading scenarios. The plastic deformations occur at the end section of the beams. Moreover, since the slab and the beams work together to form the energy dissipation mechanism, it is observed that the presence of the slab influences the length of the plastic region. However, due to the fact that the beams are very flexible, the model cannot be further used for testing on the shake table since it is not a representative model for the current design practice.

On the other hand, the M_5 model with rigid longitudinal beams exhibits the most unfavourable seismic response from the considered models. The so called "beam-slab-node" rigid block leads to the occurrence of plastic deformations, concrete cracking and longitudinal reinforcement yielding, towards the end of the columns. Therefore, the desired energy dissipation mechanism specified in the seismic design norms cannot be obtained.

Consequently, the best model to be used in the subsequent experimental tests on the shake table is the K_5 model for which the beams were designed based on the 1/12L condition. The research should be further extended to investigating the influence of the beam longitudinal reinforcement ratio on the seismic behaviour of RC moment resisting frame structures.

REFERENCES

Almahmood H., Ashour A., Sheehan T., *Flexural Behaviour of Hybrid Steel-GFRP Reinforced Concrete Continuous T-Beams,* Composite Structures, **254**, 112802 (2020).

ATENA software, http://www.cervenka.cz.

Ayensa A., Oller E., Beltran B., Ibarz E., Mari A., Gracia L., *Influence of the Flanges width and Thickness on the Shear Strength of Reinforced Concrete Beams with T-Shaped Cross Section*, Engineering Structures, **188**, 506-518 (2019).

Bednarski L., Sienko R., Howiacki T., *Analysis of Rheological Phenomena in Reinforced Concrete Cross-Section of Redzinski Bridge Pylon Based on in situ Measurements*, 7th Scientific-Technical Conference Material Problems in Civil Engineering, MATBUD' 2015, Procedia Engineering **108**, 536-543 (2015).

Birely A.C., Lowes L.N., Lehman D.E., *A Model for the Practical Nonlinear Analysis of Reinforced-Concrete Frames Including Joint Flexibility*, Engineering Structures, **34**, 455-465 (2012).

Bitencourt Jr. L.A.G., Manzoli O.L., Trindade Y.T., Rodrigues E.A., Dias-da-Costa D., *Modeling Reinforced Concrete Structures Using Coupling Finite Elements for Discrete Representation of Reinforcements*, Finite Elements in Analysis and Design, **149**, 32-44 (2018).

Budescu M., Ciongradi I., *Inginerie Seismică*, Ed. Politehnium, Iași, 2014.

Capua D., Mari A.R., *Nonlinear Analysis of Reinforced Concrete Cross-Sections Exposed to Fire*, Fire Safety Journal, **42**, 139-149 (2007).

Gao D., Gu Z., Zhu H., Huang Y., *Fatigue Behavior Assessment for Steel Fiber Reinforced Concrete Beams Through Experiment and Fatigue Prediction Model*, Structures, **27**, 1105-1117 (2020).

Gribniak V., Rimkus A., Caldentey A.P., Sokolov A., *Cracking of Concrete Prisms Reinforced with Multiple Bars in Tension-The Cover Effect*, Engineering Structures, **220**, 110979 (2020).

Hassan R.F., Jaber M.H., Al-Salim N.H., Hussein H.H., *Experimental Research on Torsional Strength of Synthetic/Steel Fiber-Reinforced Hollow Concrete Beam*, Engineering Structures, **220**, 110948 (2020).

Ishiyama Y., *Introduction to Earthquake Engineering and Seismic Codes in the World*, Hokkaido University, 2011.

Jokubaitis V., Juknevicius L., Salna R., *Conditions for Failure of Normal Section in Flexural Reinforced Concrete Beams of Rectangular Cross-Section*, 11th International Conference on Modern Building Materials, Structures and Techniques, MBMST 2013, Procedia Engineering, **57**, 466-472 (2013).

Karimipour A., Edalati M., *Shear and Flexural Performance of Low, Normal and High-Strength Concrete Beams Reinforced with Longitudinal SMA, GFRP and Steel Rebars*, Engineering Structures, **221**, 111086 (2020).

Kiss Z., Onet T., *Proiectarea structurilor de beton după SR EN 1992-1*, Ed. Abel, Cluj-Napoca, 2008.

Kripka M., Medeiros G.F., Lemonge A.C.C., *Use of Optimization for Automatic Grouping of Beam Cross-Section Dimensions in Reinforced Concrete Building Structures*, Engineering Structures, **99**, 311-318 (2015).

Leppanen J., Johansson M., Grassl P., *On the Dynamic Response of Reinforced Concrete Beams Subjected to Drop Weight Impact*, Finite Elements in Analysis and Design, **180**, 103438 (2020).

Navarro-Gomez A., Bonet J.L., *Improving the Seismic Behavior of Reinforced Concrete Moment Resisting Frames by Means of SMA Bars and Ultra-High Performance Concrete*, Engineering Structures, **197**, paper id. 109409 (2019).

Postelnicu T., *Proiectarea structurilor de beton armat în zone seismice*, MarLink, București, 2012.

Schlappal T., Kalliauer J., Vill M., Mang H.A., Eberhardsteiner J., Pichler B.L.A., *Ultimate Limits of Reinforced Concrete Hinges*, Engineering Structures, **224**, 110889 (2020).

Sciegaj A., Grassl P., Larsson F., Runesson K., Lundgren K., *Upscaling of Three-Dimensional Reinforced Concrete Representative Volume Elements to Effective Beam and Plate Models*, International Journal of Solids and Structures, **202**, 835-853 (2020).

Simao P.D., Barros H., Ferreira C.C., Marques T., *Closed-Form Moment-Curvature Relations for Reinforced Concrete Cross Sections Under Bending Moment and Axial Force*, Engineering Structures, **129**, 67-80 (2016).

Simeng L., Huixiang M., *Estimation of the Stress Level on a Cross Section of a Reinforced Concrete Beam via Acoustic Emission Intensity Distribution (AID) Analysis*, Construction and Building Materials, **164**, 463-476 (2018).

Sococol I., Mihai P., Pruteanu M., Iftode V., *Negative Influences (Effects) of Masonry Infilled RC Frames to Seismic Response of RC Frame Systems and Practical Methods (Solutions) for These Problems (State of the Art)*, Bul. Inst. Polit. Iași, s. Construction. Architecture, **65 (69)**, *4*, 21-34 (2019a).

Sococol I., Mihai P., Olteanu-Dontov I., *Ductility – Concept for Improving the Seismic Response for Structural Reinforced Concrete Frame Systems*, Bul. Inst. Polit. Iași, s. Construction. Architecture, **65 (69)**, *1*, 17-30 (2019b).

Sococol I., Mihai P., Iftode V.I., Olteanu-Dontov I., *Study Regarding the Stiffness Influence of Slab to Beams for a Plan Structural Reinforced Concrete Frame System in Seismic Zones*, Computational Civil Engineering Conference, CCE 2019, Iași, Romania, May 30th – 31th, IOP Conference Series: Materials Science and Engineering, **586** (2019c).

Sococol I., Mihai P., Toma I.O., Venghiac V.M., Olteanu-Dontov I., *Influence of Concrete Strength Class on the Plastic Hinges Location for a Reinforced Concrete Moment-Resisting Frame Structure with Consideration of the Horizontal Stiffening Effect of the Slab*, Bul. Inst. Polit. Iași, s. Construction. Architecture Section, **66 (70)**, *2*, 95-108 (2020a).

Sococol I., Mihai P., Toma I.O., Venghiac V.M., Olteanu-Dontov I., *Static Non-linear Analysis of an RC Moment Resisting Frame Structure by Considering the Longitudinal Steel Reinforcement Ratio in the Columns from the Preliminary Design Stage*, Bul. Inst. Polit. Iași, s. Construction. Architecture Section, **66 (70)**, *3*, 21-34 (2020b).

Sousa Jr. J.B.M., Muniz C.F.D.G., *Analytical Integration of Cross Section Properties for Numerical Analysis of Reinforced Concrete, Steel and Composite Frames*, Engineering Structures, **29**, 618-625 (2007).

Stratan A., *Dinamica structurilor și inginerie seismică. Note de curs*, Timișoara, 2014.

Tayeh B.A., Abu Maraq M.A., Ziara M.M., *Flexural Performance of Reinforced Concrete Beams Strengthened with Self-Compacting Concrete Jacketing and Steel Welded Wire Mesh*, Structures, **28**, 2146-2162 (2020).

Thamrin R., Kurniawan R., Melinda A.P., *Shear and Flexural Capacity of Reinforced Concrete Members with Circular Cross Section*, Sustainable Civil Engineering Structures and Construction Materials, SCESCM 2016, Procedia Engineering, **171**, 957-964 (2017).

Wang Q., Song H-L., Lu C-L., Jin L-Z., *Shear Performance of Reinforced Ultra-High Performance Concrete Rectangular Section Beams*, Structures, **27**, 1184-1194 (2020).

Yuan Y., Wang Z., *Shear Behavior of Large-Scale Concrete Beams Reinforced with CFRP Bars and Handmade Strip Stirrups*, Composite Structures, **227**, 111253 (2019).

Zidonis I., *Strength Calculation Method for Cross-Section of Reinforced Concrete Flexural Member Using Curvilinear Concrete Stress Diagram of EN-2*, 11th

International Conference on Modern Building Materials, Structures and Techniques, MBMST 2013, Procedia Engineering, **57**, 1309-1318 (2013).
*** *Cod de proiectare seismică, Partea I, Prevederi de proiectare pentru clădiri, Indicativ P100-1*, Ministerul Dezvoltării Regionale și Administrației Publice, Mai 2013.
*** *Eurocod 2: Proiectarea structurilor de beton, Partea 1-1: Reguli generale și reguli pentru clădiri, Indicativ SR EN 1992-1-1*, ASRO, București, 2006.
*** *Eurocod 8: Proiectarea structurilor pentru rezistența la cutremur, Partea 1: Reguli generale, acțiuni seismice și reguli pentru clădiri, Indicativ SR EN 1998-1*, ASRO, București, 2004.

STUDIU STATIC NELINIAR PRIVIND INFLUENȚA SECȚIUNII TRANSVERSALE A GRINZILOR ASUPRA RĂSPUNSULUI SEISMIC DISIPATIV PENTRU O STRUCTURĂ TIP CADRU DE BETON ARMAT

(Rezumat)

Răspunsul seismic teoretic (idealizat) al structurilor tip cadru de beton armat implică mecanisme de disipare a energiei seismice prin deformarea și degradarea unor zone ductile. Aceste arii (zone speciale) se doresc să apară (să se creeze) la capete de grinzi şi la capetele inferioare ale stâlpilor de la parter. În aceste condiții, mecanismul plastic global conduce la deformarea optimă a sistemului structural. Astfel, demonstrându-se în celelalte studii științifice importanța clasei superioare de beton și a procentului superior de armare longitudinală a stâlpilor asupra răspunsului seismic global pentru un sistem reprezentativ tip cadru de beton armat cu regimul de înălțime P+1E, s-a încercat prin intermediul acestui studiu analitic, să se observe influența tipului de secțiune transversală a grinzilor (principalelor elemente disipative) asupra mecanismului global de disipare a energiei seismice. În aceste condiții, s-a efectuat un calcul static neliniar cu programul ATENA pentru trei modele structurale tip cadru (reduse la scara ½) cu diferite secțiuni transversale a grinzilor (cu grinzi rigide, grinzi normale și grinzi ductile de beton armat). În final, s-a constatat că grinzile ductile prezintă cel mai favorabil răspuns seismic lateral.